Reducing Cold-Start Emissions by Microwave-Based Catalyst Heating: Simulation Studies

V. Malashchuk[1] · S. Walter[1] · M. Engler[2] · G. Hagen[1] · G. Link[2] · J. Jelonnek[2] · F. Raß[3] · R. Moos[1]

Abstract
During cold start of vehicles with gasoline combustion engines, conversion of pollutants in the exhaust gas to inert products is very low due to low catalyst temperature. Only above the light-off temperature, significant conversion can be achieved. Previous strategies to reduce cold-start emissions have been focused on developing catalysts with a low light-off temperature. Electric catalyst heating systems have also been discussed repeatedly. A disadvantage of such systems is the required volume flow through the catalyst, which is necessary for heat transfer to the catalyst. In contrast, microwave-assisted heating allows direct introduction of thermal power into the catalyst due to dielectric losses of the catalyst materials. This work analyses simulation-based the influence of the material on the heatability by microwaves. The focus is on the substrate materials rather than the catalytically active coatings, since the substrate represents the part in the TWC where most of the dielectric losses occur. For this purpose, the temperature-dependent dielectric material properties of cordierite and silicon carbide (SiC) are investigated. The determined material properties are then transferred to a simulation model that calculates heat distribution and heat insertion based on the electromagnetic field distribution. The heat propagates better throughout the monolith due to the higher thermal conductivity of SiC compared to cordierite. In summary, SiC leads to a homogeneous heating of the entire catalyst material. The fact that dielectric losses of SiC decrease with temperature may help to self-limit the catalyst temperature.

Keywords Cold-start-emissions · Microwave resonators · Microwave heating · Simulation · Dielectric material properties

1 Introduction

Efficient exhaust gas aftertreatment systems are required to meet the stringent emission regulations of modern gasoline automobiles. Under stoichiometric conditions, the three-way catalyst (TWC) allows the conversion of pollutants, nitrogen oxides (NO_x), carbon monoxide (CO), and unburned hydrocarbons (HC) to inert products [1, 2]. The conversion is strongly temperature-dependent and is very low below the light-off temperature (50% conversion at light-off temperature) [3]. This means that most emissions occur during cold start. In this context, research in recent years has focused on optimizing the catalyst material regarding low light-off temperatures. Another approach is convective heating of the catalyst during the cold start phase, e.g., with an electrically heated catalyst (EHC) [4]. EHCs are located upstream of the catalytic converter. The exhaust gases flow through a heated metallic structure, are heated up and heats then the catalyst convectively. In [5] two electrically heated control strategies were introduced to increase the reduction of CO and NO_x at the cold start of diesel-powered engine vehicles under WLTC obligation. In a different approach, an exhaust heat recovery system (EHRS) was used in experiments to improve fuel economy and to reduce total hydrocarbon, CO and even NO_x emissions at cold start (NEDC) at − 7 °C and 25 °C [6]. A disadvantage of both systems is the dependence of the heat transfer rate on the gas flow. In [7] a novel method to trap cold start emission in a vessel until the light of temperature is reached was introduced. The simulative results of the analysis were verified

✉ R. Moos
functional.materials@uni-bayreuth.de

[1] Bayreuth Engine Research Center (BERC), Department of Functional Materials, University of Bayreuth, 95440 Bayreuth, Germany

[2] Karlsruhe Institute of Technology, IHM, 76344 Eggenstein-Leopoldshafen, Germany

[3] Honda R&D Europe (Deutschland) GmbH, 63073 Offenbach Am Main, Germany

by experiments. The results show a significant reduction of NO_x emissions but no benefit for treating the CO emissions.

Microwave-based measurement methods have been investigated in previous studies as a tool for material characterization and in the field of sensor technology. They allow for determining the oxidation state of ceria- based TWCs or the amount of sorbed ammonia in NH_3-SCR catalysts [8–11]. Operated as a sensor, determining the soot load of both diesel and gasoline particulate filters is also possible [12, 13]. For the sensor application, power in the milliwatt range is applied. The resulting low electric field strengths in the resonator chamber (i.e., in the catalyst canning) thus have no effect on the material under investigation. In contrast, this work is based on effects of strong electric fields on the material under investigation, applying power in the kilowatt range. In previous studies, heating of cordierite substrate materials, parts of a honeycomb structure, has already experimentally been shown for an applied power in the kilowatt range [14], and full cylindrical cordierite honeycomb at different diameter to length ratios have been experimentally investigated by [15].

In this work, electric field distribution at discrete excitation frequencies and the material influence on them are investigated. Both, the electric field distribution, and the local field strength depend on local dielectric material properties. Thereby, the relative permittivity influences the resonant frequencies of the resonant modes and the dielectric losses are responsible for the electric field strength. To better understand how local monolith heating contributes to the total heating of the monolith material, the model includes gas flow and heat transfer simulation. The analyses focus on the substrate materials cordierite and silicon carbide (SiC) and not on the catalytic layer of a TWC, because in real applications, the substrate material accounts for most of the mass, and hence, microwave energy is mainly converted there to heat. For the cold start phase, microwave-assisted heating of the substrate can heat the catalytically active layer in the catalyst faster compared to conventional methods. Therefore, by reaching the light-off temperature faster, emissions during the cold-start phase can be reduced.

2 Microwave-Based Heating

By microwave-based heating, electromagnetic energy is transferred in the material and converted into thermal energy. This conversion of energy depends both on the dielectric losses of the material and the electric field strength. If a dielectric material is placed in a closed cavity resonator with conductive walls, the local electric field strength can be changed by changing the geometry of the resonator and the excitation frequency of the electromagnetic waves. At so-called resonant frequencies, standing waves with local maxima and minima of the electric field strength occur in the resonator. These specific states of electric field distribution associated with corresponding resonant frequencies are denoted as modes [16].

Since for microwave-based heating, electromagnetic energy is dissipated directly inside a material, it leads, in contrast to other heating methods, to a volumetric heating of the material. The power loss density P_l follows Eq. (1):

$$P_l = \sigma |E|^2 + \varepsilon_0 \varepsilon_r'' \omega |E|^2 \tag{1}$$

The first term corresponds to conductive losses due to the transport of free charge carriers and depends on the material conductivity σ and the absolute value of the electric field E [17]. The second depends on the vacuum permittivity ε_0, the dielectric losses ε_r'', the angular frequency ω (which is related to the frequency by $\omega = 2\pi f$), and the absolute value of the electric field strength E. The losses are caused by various polarization mechanisms inside the material [17]. In this work, both loss mechanisms contribute to the energy dissipation.

3 Dielectric Properties of Catalyst Substrates

The dielectric properties of cordierite and silicon carbide are experimentally determined by the cavity perturbation method. The samples were placed in a cavity resonator. From the analysis of the resonant frequency f_s and the reciprocal quality factor Q_s^{-1} at approximately 1.2 GHz at the TM_{010} mode, the permittivity ε_r' and the loss factor ε_r'' were calculated. The reciprocal quality factor describes the ratio of dissipated energy to the energy that is stored in the system per oscillation cycle. The reciprocal quality factor Q_s^{-1} is a measure for losses occurring in the resonator. Thus, this parameter is directly related to dielectric losses of the material in the resonator [18]. By comparing the empty resonator and the resonator filled with sample, the dielectric material properties of the sample can be determined. This relationship is represented by Eqs. (2) and (3). In Eq. (2), the measured resonant frequency difference Δf_s between empty and with sample loaded resonator is proportional to the permittivity ε_r'. Eq. (3) shows the same dependency between the difference in the reciprocal quality factor ΔQ_s^{-1} and the loss factor ε_r'' [16, 17].

$$\Delta f_s \propto \varepsilon' \tag{2}$$

$$\Delta Q_s^{-1} \propto \varepsilon'' \tag{3}$$

The setup and the procedure therefore can be found in [19, 20]. Since powder-air mixtures instead of bulk samples

are investigated, only effective material properties can be determined with this measurement method.

Figure 1 shows the results of the experimental analysis. For both materials, the air content was eliminated. Therefore, the dielectric properties for the bulk materials are displayed. Figure 1a depicts the permittivity ε' versus temperature for both materials. At room temperature, the value for SiC is about 22 and for cordierite 3.3. Almost no temperature dependency occurs. In Fig. 1b, the dielectric losses are plotted against temperature. They are strongly but differently temperature-dependent. At room temperature, the dielectric losses of SiC are high, however they decrease with increasing temperature. Conversely, for cordierite, the dielectric losses are low at room temperature and increase with increasing temperature. At a temperature of about 500 °C, the losses of both materials are equal.

In terms of microwave-assisted heating, this means that the higher dielectric losses of SiC compared to cordierite at room temperature yield a higher heat dissipation in SiC and the material can be heated faster. As the temperature increases, the dielectric losses of SiC decrease. Since in contrast, the dielectric losses of cordierite continuously increase. At constant electrical field, this may lead to the formation of local hot spots and to material failure due to thermal stresses.

4 Simulative Determination of the Influence on the Heating Characteristics

In the following, a simulation model (COMSOL Multiphysics® 5.6) is used to analyze the heating behavior of the monolith substrate by microwaves. Figure 2 depicts a sectional view of the three-dimensional simulation model. In the center of the metallic canning, the catalyst monolith is located. For both materials used in the analysis, the dimensions in the model are kept constant. The diameter of the gas inlet and outlet part of the cavity is 50 mm and the length is 45 mm. The main body part of the canning, where the monolith is located, has a diameter of 132 mm and a length of 135 mm. The length of the entire canning is 315 mm. In the model, the monolith has a diameter of 118 mm (4.66 inch) a length of 90 mm. The resulting monolith volume is 1 L. The fiber mat between the monolith and the canning is assumed lossless with a relative permittivity of 3. For coupling the electromagnetic field, a coaxial feed is used in the front part of the resonator cavity. All metal surfaces in the simulation are defined with the impedance boundary condition (electrical conductivity $\sigma \approx 4 \times 10^6$ S/m) to include the skin depth of electromagnetic waves in the simulation. For the simulative analysis, the catalyst is meshed with triangular prisms. The remaining regions of the model are meshed with tetrahedrons created using the COMSOL settings for a "fine" mesh. The mesh has a total number of 14,602 volume elements.

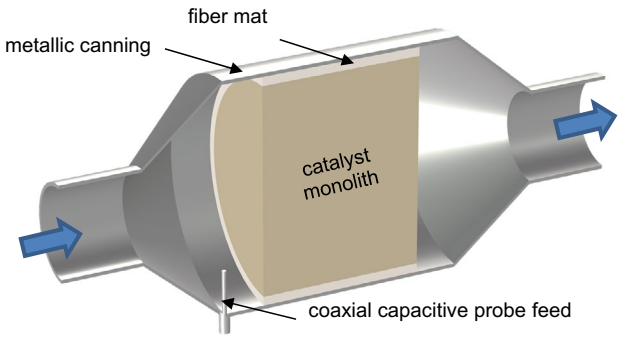

Fig. 2 The three-dimensional model consisting of the metallic canning, catalyst monolith, fiber mat, and antenna (coaxial-capacitive probe feed)

To define the dielectric material properties of the monolith, the data from Fig. 1 are used. The air content in the monolith was taken into account. For calculation, a density of rectangular cells of 600 cpsi (93 cells per cm^2) and a wall thickness of 3.5 mil (0.089 mm) were assumed.

During the simulation of the electric field distribution, a power of 10 kW was applied to the antenna for each

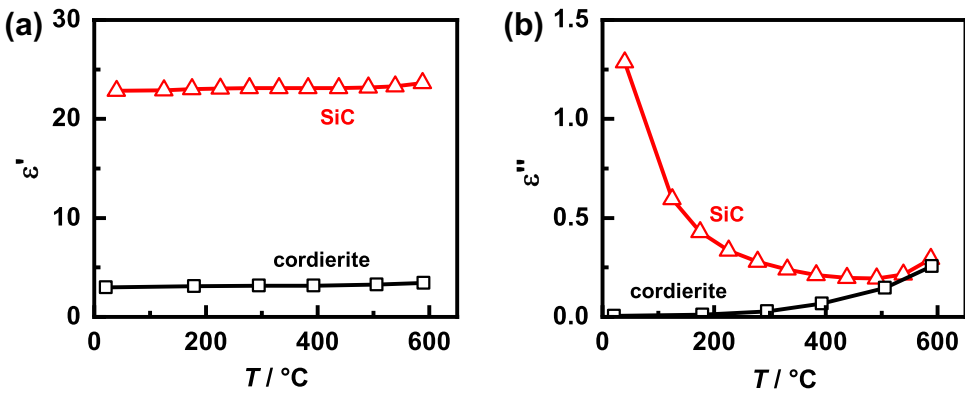

Fig. 1 **a** Influence of temperature on the permittivity ε' and **b** of the dielectric losses ε'' of SiC and cordierite

excitation frequency. From the simulated three-dimensional electric field distributions, the local heating power was derived. This was considered in the calculation for the heat distribution inside the substrate material and the heat transfer to the environment through the canning and fiber mat. By coupling the heat distribution results with the two-dimensional flow model, also the exhaust gas temperature was calculated. The flow model and the simulation of the convective heat transport have been described in detail in a previous study [12]. The calculation of the transient heating process was done using COMSOL's Backward Differentiation Formula (BDF) solver with a free choice of the length of the timesteps. At the beginning of the simulation, the temperature was set to 20 °C for all elements. The exhaust gas flow was assumed to be fully developed with a constant mass flow of 50 kg/h and an inlet gas temperature of 20 °C (worst case estimation as this leads to no additional heating of the catalyst). Both are assigned to the exhaust gas duct before the widening of the catalyst canning. Since no additional heat sources are present upstream of the catalyst, the catalyst inlet temperature is also 20 °C during the entire heating process. Constant thermal conductivities of 2.5 W/(mK) for cordierite and 80 W/(mK) for SiC were assumed [21, 22].

5 Results and Discussion

Local heating requires high electric field strengths, which only occur at resonances. At the same time, the electric field distribution is important with respect to the heat distribution in the monolith. For this reason, an excitation frequency in the range between 2.3 and 2.7 GHz was investigated for both materials in the first step of the analysis. Figure 3 shows the results at the starting temperature of the simulation (20 °C). Figure 3a depicts the heating power dissipated into the cordierite substrate. At the resonance of 2.595 GHz, the heating power dissipated in the material is only about 0.06 kW. Figure 3b shows the results for the SiC monolith. Here, at a frequency of 2.66 GHz about 9.5 kW are dissipated in the material. Apart from the scaling of the y-axes, both spectra look differently. The reason therefore is the different effective relative permittivity of both materials (1.34 for cordierite and 4.18 for SiC), in conjunction with the different dielectric loss factors at 20 °C. As shown in Fig. 1, the dielectric losses of SiC at 20 °C are high and those of cordierite are low.

The different spectra, as shown in Fig. 3 come along with a different electric field distribution. For the cordierite monolith excited at the resonant frequency of 2.595 GHz, Fig. 4a

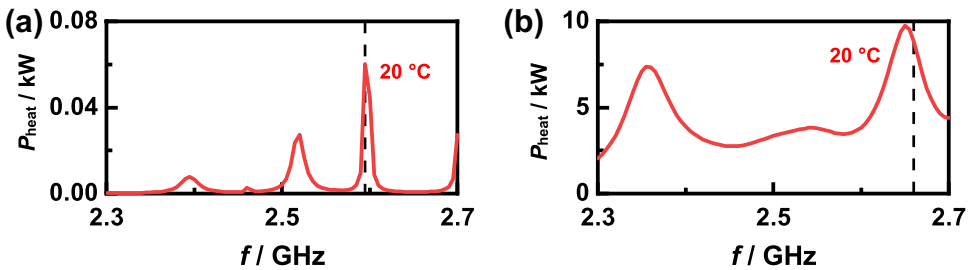

Fig. 3 Heating power at temperature of 20 °C in the frequency range between 2.3 and 2.7 GHz for **a** cordierite, and **b** SiC. Excitation power is 10 kW. The very low heating power for the cordierite originates from the low dielectric losses at room temperature (Fig. 1a). Due to the high dielectric losses of SiC at 20 °C (Fig. 1b), the electrically coupled power dissipates almost completely and heats the catalyst in the resonance at 2.66 GHz. Please note the different axis scaling

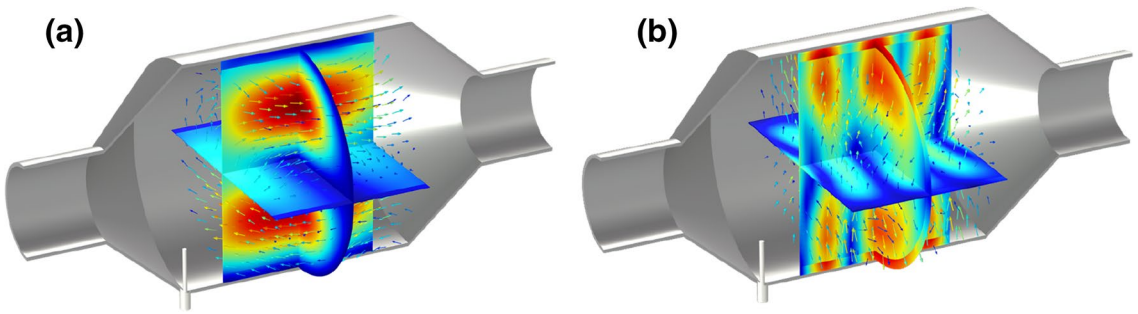

Fig. 4 Electric field distribution at room 20 °C of cordierite (**a**) and SiC (**b**). Red areas represent high electric field strength. Where the electric field strength is high, local heating occurs. Excitation frequencies are 2.595 GHz for the cordierite catalyst and 2.66 GHz for the SiC catalyst

shows the resulting electric field distribution. In Fig. 4b, the resulting electric field distribution for the SiC monolith at 2.66 GHz is shown. Areas marked in red (blue) indicate high (low) electric field strength.

Since the permittivity for both materials does not depend on temperature, (cf. Fig. 1a), the electric field distribution in the monolith does not change when the material is heated. The electric field strength, however, changes due to the changes in the dielectric losses (cf. Fig. 1b). In general, electric field strengths in materials with high dielectric losses are lower than in materials with low dielectric losses.

In the following analysis, the excitation frequencies were kept constant (2.595 GHz for the cordierite monolith and 2.66 GHz for the SiC monolith). With time, the materials heat up. Figure 5a shows the temperature profile of the maximum temperature and of the average temperature of the cordierite monolith. The mean temperature shows hardly any temperature increase over time. The calculation was stopped as soon as temperature > 500 °C was reached. This value is then no longer evaluated. At the last evaluated time step (113 s), the local maximum temperature is approx. 400 °C. Figure 6a shows the corresponding temperature distribution in the monolith just before the rapid rise of the maximum temperature at 110 s. At the hotspot, the temperature has increased, but the heat has not distributed over the entire monolith. The low thermal conductivity of cordierite is the main reason for this. Comparing Figs. 4a and 6a elucidates that the hotspots form at local points of high electric field strength and the increasing dielectric losses with increasing temperature are responsible for the locally absorbed power.

On Fig. 5b, the average and maximum temperatures for the SiC monolith are plotted versus time. Starting also at the initial temperature of 20 °C, the maximum and average temperatures increase and approach asymptotically constant values. At 110 s, the mean temperature of the SiC monolith reaches 500 °C and the maximum temperature is only slightly higher at about 600 °C. The corresponding temperature distribution in the monolith is shown in Fig. 6b. Here, a uniform heat distribution over the monolith is observed and no hotspots occur. Unlike cordierite, SiC has a high thermal conductivity. Thus, the heat spreads faster over the entire monolith. Dielectric losses also decrease with temperature. Locally, this reduces the ability of the material to absorb thermal power.

6 Conclusion

Since the substrate of catalytic monoliths dominates the catalyst in terms of mass, microwave-assisted heating of the substrate materials was analyzed in this work. For this purpose, the dielectric constant and the dielectric losses of SiC and cordierite were experimentally determined in the range of 25–600 °C. Subsequently, the dielectric material properties were used to define a 1ltr catalyst monolith in a simulation model. The purpose of the simulation was to investigate the influence of the local heating distribution in the monolith due to the local changes in dielectric material properties caused by the local changes in temperature.

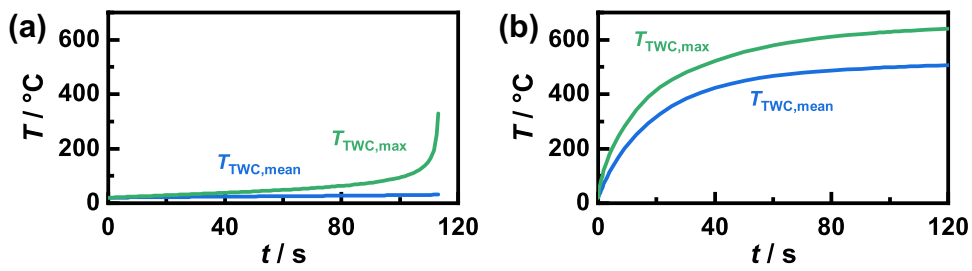

Fig. 5 Time course of monolith mean and local maximum temperature for **a** cordierite and **b** SiC catalysts. Excitation power 10 kW

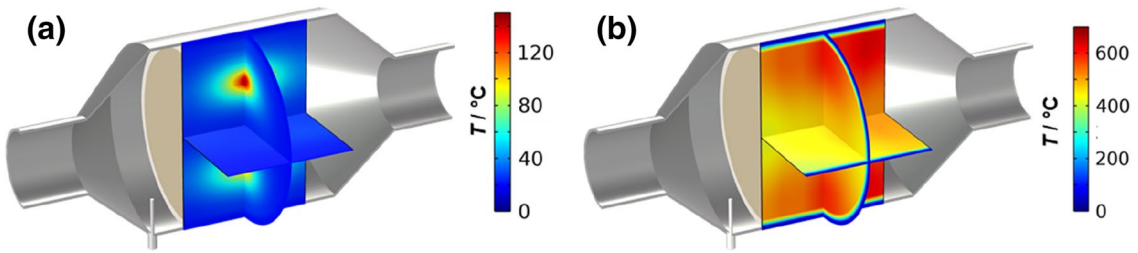

Fig. 6 Temperature distribution for **a** cordierite and for **b** SiC catalyst at 110 s. Excitation frequency for the cordierite catalyst is 2.595 GHz and for the SiC catalyst is 2.66 GHz. Excitation power for both materials was set constant to 10 kW

Compared to cordierite, SiC has high dielectric losses at room temperature. This makes SiC more appropriate for microwave heating. The dielectric losses of SiC material decrease with temperature, while they increase for cordierite. The heat propagates better throughout the monolith due to the higher thermal conductivity of SiC compared to cordierite. In summary, this leads to more homogeneous heating of the entire catalyst material. The fact that dielectric losses of SiC decrease with temperature may help to self-limit the catalyst temperature.

With SiC as a catalyst substrate material, an average temperature of about 400 °C can be reached in about 120 s (worst case with constant inlet temperature of 20 °C). It should be mentioned that 400 °C is above the typical light-off temperature of TWCs. When reaching the light-off temperature, the exothermic catalytic reaction additionally heats the catalyst. Such effects were not considered in the here-shown model.

From an industrial point of view, the microwave-assisted catalyst heating as a new technology in automotive industry competes with established exhaust gas heating technologies that are currently less expensive compared to the application of a microwave-based catalyst heating. These up-costs are expected to get reduced during mass production, but will most likely remain above the costs for, e.g., electrically heated catalysts. However, the ability to pre-heat the microwave assisted catalyst system before engine start might justify these up-costs in the future.

References

1. Winkler M, Grimm J, Lenga H, Min B-H (2014) Gasoline engine combustion development for EU 6c emission legislation. In: Liebl J (ed) Internationaler Motorenkongress 2014. Springer Vieweg, Wiesbaden
2. Lox E, Engler B (1999) Environmental catalysis - mobile sources. In: Ertl G, Knözinger H, Weitkamp J (eds) Environmental catalysis. Wiley-VCH, Weinheim
3. Reif K (2015) Abgastechnik für Verbrennungsmotoren. Springer Fachmedien, Wiesbaden
4. van Basshuysen R, Schäfer F (2015) Handbuch Verbrennungsmotor. Springer Fachmedien, Wiesbaden
5. Gao J, Tian T, Sorniotti A (2017) On the emission reduction through the application of an electrically heated catalyst to a diesel vehicle. Energy Sci Eng 7:2383–2397. https://doi.org/10.1002/ese3.416
6. Shen K, Chang I, Chen H, Zhang Z, Wang B, Wang Y (2019) Experimental study on the effects of exhaust heat recovery system (EHRS) on vehicle fuel economy and emissions under cold start new European driving cycle (NEDC). Energy Convers Manag 197:111893–111902. https://doi.org/10.1016/j.enconman.2019.111893
7. Teymoori MM, Chitsaz I, Kashani NA, Davazdah Emami M (2022) Cold-start emission reduction of the gasoline-powered vehicle utilizing a novel method. Int J Engine Res. https://doi.org/10.1177/14680874221100816
8. Steiner C, Gänzler AM, Zehentbauer M et al (2019) Oxidation state and dielectric properties of ceria-based catalysts by complementary microwave cavity perturbation and X-ray absorption spectroscopy measurements. Top Catal 62:227–236. https://doi.org/10.1007/s11244-018-1110-3
9. Steiner C, Malashchuk V, Kubinski D et al (2019) Catalyst state diagnosis of three-way catalytic converters using different resonance parameters-a microwave cavity perturbation study. Sensors 19:3559–3573. https://doi.org/10.3390/s19163559
10. Rauch D, Dietrich M, Simons T et al (2017) Microwave cavity perturbation studies on H-form and Cu ion-exchanged SCR catalyst materials: correlation of ammonia storage and dielectric properties. Top Catal 60:243–249. https://doi.org/10.1007/s11244-016-0605-z
11. Dietrich M, Rauch D, Simon U et al (2015) Ammonia storage studies on H-ZSM-5 zeolites by microwave cavity perturbation: correlation of dielectric properties with ammonia storage. J Sens Sens Syst 4:263–269. https://doi.org/10.5194/jsss-4-263-2015
12. Walter S, Schwanzer P, Hagen G et al (2020) Modelling the influence of different soot types on the radio-frequency-based load detection of gasoline particulate filters. Sensors 20:2659–2678. https://doi.org/10.3390/s20092659
13. Feulner M, Hagen G, Piontkowski A et al (2013) In-operation monitoring of the soot load of diesel particulate filters: initial tests. Top Catal 56:483–488. https://doi.org/10.1007/s11244-013-0002-9
14. Marin R, Savu S (2020) Microwave heating of cordierite ceramic substrate for after treatment systems. Ann "Dunarea de Jos" Univ Galati 31:23–29. https://doi.org/10.35219/awet.2020.03
15. Marin R, Olei A, Stefan I, Savu I, Ghelsingher C, Savu S, David A (2021) Research on microwave heating conditions of cordierite cylindrical shape for after treatment applications. Acta Technica Napocensis 64:377–386. https://doi.org/10.35219/awet.2020.03
16. Pozar DM (2012) Microwave engineering, 4th edn. Wiley, Hoboken
17. Mehdizadeh M (2009) Microwave/RF applicators and probes for material heating, sensing, and plasma generation: a design guide. William Andrew, Norwich
18. Chen L (2005) Microwave electronics: measurement and materials characterization. Wiley, Chichester
19. Steiner C, Walter S, Malashchuk V et al (2020) Determination of the dielectric properties of storage materials for exhaust gas aftertreatment using the microwave cavity perturbation method. Sensors 20:6024–6041. https://doi.org/10.3390/s20216024
20. Dietrich M, Rauch D, Porch A et al (2014) A laboratory test setup for in situ measurements of the dielectric properties of catalyst powder samples under reaction conditions by microwave cavity perturbation: set up and initial tests. Sensors 14:16856–16868. https://doi.org/10.3390/s140916856
21. Kollenberg W (ed) (2009) Technische Keramik: Grundlagen, Werkstoffe, Verfahrenstechnik. Vulkan-Verl, Essen
22. Zuberi B, Liu J, Pillai S, Weinstein J et al (2008) Advanced high porosity ceramic honeycomb wall flow filters. SAE Technical Paper 2008-01-0623. https://doi.org/10.4271/2008-01-0623